Clays and Clay Minerals, Vol. 50, No. 2, 208-216, 2002.

RAPID AND QUANTITATIVE MEASUREMENT OF HEMATITE AND GOETHITE IN THE CHINESE LOESS-PALEOSOL SEQUENCE BY DIFFUSE REFLECTANCE SPECTROSCOPY

JUNFENG JI[1]*, WILLIAM BALSAM[2], JUN CHEN[1] AND LIANWEN LIU[1]

Institute of Surficial Geochemistry, State Key Laboratory of Mineral Deposit Research, Department of Earth Sciences, Nanjing University, Nanjing 210093, China
[2] Department of Geology, University of Texas at Arlington, Arlington, TX 76019, USA

Abstract—The long, continuous deposition of dust in the Chinese loess plateau offers a unique opportunity to study the nature of Fe oxide formation in a wide range of climatic conditions. A technique to obtain quantitative estimates of the concentration of hematite and goethite in loess and paleosol samples is reported. Experiments using diffuse reflectance spectroscopy on sets of laboratory mixed and natural loess and paleosol samples show that it is possible to obtain rapid and quantitative estimates of the absolute concentration of hematite and goethite in the Chinese loess sediments. Typical loess and paleosol samples were deferrated using the CBD procedure to produce a natural matrix material to which hematite and goethite in known weight percentages were added to produce a set of calibration standards. Spectral violet, blue, green, yellow, orange, red and brightness of standards were calculated from the reflectance data and served as independent variables for a multiple linear regression analysis. The effect of changing matrix from loess to paleosol was overcome by including a variety of different loess and paleosol samples in the regression equations. The resulting calibration equations provide estimates of wt.% hematite and goethite and have correlation coefficients >0.93. The total measured hematite and goethite concentrations exhibited consistent variations with CBD extractable iron. Tests of the equations for buffering changes in matrix composition were run with samples of varying mineralogical composition (calcite, illite, *etc.)* and demonstrated that the equations are well buffered for changes in matrix composition from loess to paleosol.
Key Words—Diffuse Reflectance Spectroscopy, Goethite, Hematite, Loess, Multiple Regression.

INTRODUCTION

Changing color is one of the most striking features of Northern mid-latitudes loess-paleosol sequences; the loess is light yellow and the interstratified paleosol reddish brown. The alternation of paleosol and loess units in the Loess Plateau records a succession of important environmental changes, with intervals of high dust influx alternating with intervals marked by lower dust influx and enhanced pedogenesis (An *et al.,* 1990, 1991). Even though color has been used as a descriptor of the loess profile and many generalizations have been drawn from color determinations (Liu, 1985; Kukla and An, 1989; Porter, 2000), the concentration of goethite and hematite responsible for these color variations in the loess sequence, has never been determined; the magnetic Fe oxide minerals in loess sequences, however, have been well studied mainly by magnetic measurement and Mossbauer analysis in combination with citrate-bicarbonate-dithionite (CBD) treatment (Heller *et al,* 1993; Verosub *etal.,* 1993; Heller and Evans, 1995; Fine *et al,* 1995; Liu *et al,* 1999; Vidic *et al,* 2000). This lack of information concerning hematite and goethite probably results from difficulty identifying these minerals at the low concentrations typical of soils and sediments with standard techniques. Under optimal circumstances the detection limit of X-ray diffraction (XRD) for hematite or goethite is ~1 wt.%. Mossbauer spectrometry provides the relative proportion of Fe phases and is rather time consuming. Selective chemical extraction techniques are slow and analytically difficult, and do not distinguish hematite from goethite. The combination of CBD-extracted Fe and oxalate-extractable Fe has been commonly used to get an independent estimate of crystalline Fe (hydr) oxides in soils, but it cannot be used to estimate the amount of hematite and goethite in the Chinese loess samples because of the common presence of much fine-grained maghemite (Verosub *et al.,* 1993; Fine *et al,* 1995; Liu *et al,* 1999).

Diffuse reflectance spectroscopy is especially sensitive to Fe oxides and oxyhydroxides in soils and sediments and has been used as an ancillary method to identify and estimate Fe oxides in soils and sediments (Kosmas *et al,* 1986; Fernandez, 1988; Deaton and Balsam, 1991; Torrent and Barron, 1993; Malengreau *et al,* 1994; Cornell and Schwertmann, 1996; Scheinost *et al,* 1998). The most frequently used aspects of reflectance spectra as an indicator of Fe oxides include soil color (Torrent *et al,* 1983; Barron and Torrent, 1986; Barron and Montealegre, 1986; Scheinost and Schwertmann, 1999), first and/or second derivatives of the reflectance spectrum (Kosmas *et al,* 1986; Deaton and Balsam, 1991; Malengreau *et al,* 1994; Scheinost *et*

* E-mail address of corresponding author: jijunfep@jlonline.com

al., 1998) and factor analysis (Balsam and Deaton, 1991; Harris and Mix, 1999). In the past, the matrix effect has impeded the quantitative estimate of Fe oxides in soils and sediments by spectral analysis. For example, as described by Deaton and Balsam (1991), the height of the first peak for both hematite and goethite is a function of the concentration of the Fe oxide minerals and the nature of the matrix. If the matrix composition remains constant then peak height is a reasonable indicator of Fe oxide concentration. However, peak height may change as matrix composition changes.

Because the composition of loess and paleosols differs – loess has a higher concentration of carbonate and lower concentration of clay minerals – any technique that provides a quantitative estimate of Fe oxide concentration from the loess sequence must take these compositional differences into account. In this paper we present details of a new procedure to estimate quantitatively hematite and goethite concentration in the loess sequence by visible light diffuse reflectance spectroscopy.

EXPERIMENTAL TECHNIQUES

Calibration samples

Quantitative estimation of mineral concentration in geological samples from reflectance spectra requires a set of calibration samples with known quantities of minerals to be estimated. In order to minimize the matrix effect, the matrices of the calibration samples should be similar to those of the measured samples (Deaton and Balsam, 1991; Balsam and Deaton, 1996), in this case loess and paleosol material. Typically, the matrix of the calibration samples is prepared in the laboratory by mixing minerals characteristic of the area of interest. Two problems are associated with preparing matrix materials. First, it is difficult to identify the range of components present in possible matrices. No single mixture can encompass all the variability present in natural materials. Second, sediment components that are in concentrations too low to be identified by standard techniques, XRD for example, may be spectrally very important (Deaton and Balsam, 1991). For these reasons we have taken another approach. Our goal was to estimate the concentration of hematite and goethite in paleosol and loess samples. We obtained calibration samples by first removing (deferrating) hematite and goethite from selected loess and paleosol samples thereby providing a natural matrix material. Then, known quantities of pigment-grade hematite and goethite were added back to the deferrated matrix material to produce our calibration samples or standards (Table 1). The method of deferrating soil and then adding synthetic hematite and goethite was used by Scheinost *et al.* (1998) to obtain an index of the band intensity in the second-derivative spectra for goethite and hematite and to estimate the hematite/(hematite+goethite) ratio. Our standards, therefore, contain actual loess and paleosol matrix material to which known quantities of hematite and goethite have been admixed. By using this approach we

Table 1. Wt.% of hematite and goethite in calibration samples or standards.

Sample number[1]	Hematite (%)	Goethite (%)	%Violet	%Blue	%Green	%Yellow	%Orange	%Red	Brightness
1	0.50	0.00	10.25	9.01	16.37	12.77	19.60	32.00	835
2	0.25	0.00	11.66	10.54	18.97	12.67	17.71	28.45	928
3	0.25	0.25	10.98	10.21	19.24	12.95	17.88	28.74	900
4	0.25	0.40	10.61	9.73	18.57	13.09	18.41	29.60	930
5	0.10	0.25	11.75	11.21	21.06	12.70	16.62	26.66	1005
6	0.10	0.40	11.31	10.84	20.87	12.96	16.97	27.05	952
7	0.10	0.50	11.02	10.77	21.10	13.01	16.94	27.16	1049
8	0.10	0.60	10.44	10.09	20.56	13.38	17.56	27.97	983
9	0.10	0.00	12.93	11.85	20.87	12.30	16.21	25.84	1035
10	0.05	0.00	13.24	12.50	21.95	12.09	15.50	24.72	1033
11	0.00	0.50	11.77	11.44	22.44	12.86	16.04	25.44	1031
12	0.00	1.00	10.11	10.13	21.97	13.64	17.06	27.08	1006
13	0.00	2.00	9.10	8.78	20.38	13.98	17.99	29.78	666
14	0.25	1.50	8.95	8.59	18.58	13.52	18.75	31.60	740
15	0.22	1.37	9.11	8.66	18.47	13.50	18.72	31.53	734
16	0.25	1.25	9.16	8.66	18.36	13.41	18.75	31.66	747
17	0.00	1.00	10.31	9.76	20.80	13.25	17.11	28.78	599
18	0.25	1.00	10.11	9.28	18.35	13.05	18.38	30.82	604
19	0.00	0.50	11.59	10.76	21.05	12.44	16.24	27.91	556
20	0.25	0.50	10.83	9.66	18.07	12.68	18.13	30.63	560
21	0.15	0.50	10.58	10.19	19.91	12.78	17.37	29.16	753
22	0.10	0.00	12.58	11.32	20.00	12.01	16.33	27.76	585
23	0.05	0.00	13.09	11.80	20.72	11.75	15.69	26.95	569
24	0.50	0.00	10.04	8.32	14.26	11.78	19.88	35.72	494
25	0.00	0.00	13.61	12.49	21.79	11.56	14.98	25.57	576

[1] 1–12: deferrated loess matrix; 13–25: deferrated paleosol matrix

hope to write regression equations for loess and paleosol materials.

The results of this study clearly depend on how closely the synthetic hematite and goethite pigments we used as standards resemble the natural Fe oxides. For the hematite standard we used Pfizer R1599, pure red Fe oxide, and for goethite we used Hoover Color Corporation Synox HY610 yellow. Both standards are fine-grained, *i.e.* micron or sub-micron powders, similar in size to Fe oxides found in soil (Bigham *et al.*, 1978). According to chemical information provided by the manufacturer, both the standards are chemically correct for hematite and goethite, and XRD results (Deaton and Balsam, 1991) indicate the appropriate crystallography. We used synthetic hematite and goethite for two reasons. First, natural samples are highly variable and are generally mixed with other Fe oxide minerals. The consistency provided by synthetic samples provides a baseline for modeling experiments. Second, the spectral patterns produced by the synthetic Fe oxides have been observed in many natural samples including those from the deep sea (Barranco *et al.*, 1989; Balsam and Deaton, 1991; Balsam and Wolhart, 1993), dust on atmospheric filters (Arimoto *et al.*, 2000), soils (Scheinost *et al.*, 1998; Scheinost and Schwertmann, 1999) and Loess Plateau sediments (Balsam and Ji, 1999). Nevertheless, natural Fe oxides present a problem for modeling because metals other than Fe may be incorporated into the crystal structure. In some cases the substituted metals may change the color (see for example Schwertmann and Cornell, 1991) and could cause our equations to underestimate either hematite or goethite concentration.

Our calibration database consisted of 25 samples, 12 deferrated loess samples and 13 deferrated paleosol samples into which hematite and goethite were added. The amount of hematite and goethite mixed into these deferrated samples was based on previous mixing experiments (Balsam and Ji, 1999). Hematite, a powerful coloring agent, was mixed in concentrations that ranged from 0 to 0.5 wt.%, whereas goethite, not as significant a coloring agent as hematite, was mixed in concentrations that ranged from 0 to 2.0 wt.%.

Citrate-bicarbonate-dithionite (CBD) procedure

Loess and paleosol samples were deferrated by the CBD method for removing pedogenic Fe oxides from clays (Mehra and Jackson, 1960; Verosub *et al.*, 1993; Fine *et al.*, 1995; Hunt *et al.*, 1995). Samples were extracted twice with sodium dithionite in hot (75°C) sodium citrate and sodium bicarbonate solution to ensure complete removal of pedogenic Fe oxides. The CBD soluble Fe (% Fe_2O_3) was determined on a JY38S inductively coupled plasma spectrometer.

Spectral reflectance measurements

Reflectance spectra of samples were analyzed in a Perkin-Elmer Lambda 6 spectrophotometer with a diffuse reflectance attachment (reflectance sphere) from 250–850 nm, *i.e.* from the near ultra-violet (NUV: 250–400 nm), through the visible (VIS: 400–700 nm), and into the near infrared (NIR: 700–850 nm). Sample preparation and analysis followed procedures described in Balsam and Deaton (1991). Ground samples were made into a slurry on a glass microslide with distilled water, smoothed, and dried slowly at low temperature (<40°C). Data, reflectance intensity relative to a white barium sulfate standard, are written directly to a computer disk at 1 nm intervals. Reflectance data were processed to obtain percent reflectance in standard color bands (Judd and Wyszecki, 1975), *i.e.* violet = 400–450 nm, blue = 450–490 nm, green = 490–560 nm, yellow = 560–590 nm, orange = 590–630 nm, red = 630–700 nm. Percent reflectance in the standard color bands was calculated by dividing the percentage of reflectance in a color band by the total reflectance in a sample. Total reflectance of a sample or brightness (Balsam *et al.*, 1999) is calculated by summing a sample's reflectance values from 400–700 nm. Because we have sampled the spectrum at 10 nm intervals, where the bands overlap half the reflectance value goes to one band and half to the other. No other data transforms were applied to the raw spectral data. Data processing was restricted to the visible because this is the region of the spectrum most sensitive to the Fe oxide minerals (Deaton and Balsam, 1991) responsible for color differences in the loess sequence.

Percentage carbonate measurements

Weight percent carbonate was determined using the vacuum gasometric technique described by Jones and Kaiteris (1983) with a precision of $\pm 0.25\%$. Samples were ground to <38 μm and dried for at least 10 h at 50°C. About 0.2 g of ground sample was reacted under vacuum with 5 ml of concentrated (85%) phosphoric acid for 1.25 h. Pressure generated by the reaction was measured on a pressure measurement manifold. Weight percent carbonate was calculated by comparing the pressure generated by the sample to pure $CaCO_3$ after correcting for temperature and atmospheric pressure.

Multiple regression

There are many ways to relate independent variables (percent reflectance in standard color bands or spectral values at specified wavelengths) to dependent variables (analytically determined component values such as hematite and goethtite to be estimated from spectra). The simplest model relates a single independent variable to the dependent variable by linear regression, such as redness to hematite concentration. For natural materials a single independent variable does not generally provide an adequate model; rather, the combined influence of several independent variables usually improves estimates of the dependent variable. A multiple regression,

therefore, is more appropriate for relating spectral wavelengths to sediment components (Balsam and Deaton, 1996). For our calibration data set a multiple linear regression model was sufficient to explain most of the variability. As with any regression model, results are only reliable where the equation is interpolating, *i.e.* between the minimum and maximum values of the dependent variables in the calibration database. This means our regression equation should be most accurate for 0–0.5% hematite and 0–2.0% goethite by weight. All regressions were performed using SPSS for Windows.

RESULTS AND DISCUSSION

Calibration equations

Our multiple linear regression model for both hematite and goethite began with seven independent variables, including spectral violet, blue, green, yellow, orange, red and brightness. The choice of independent variables to include in a calibration equation was produced using a step-wise multiple regression. A summary of the multiple regression statistics and parameter estimates of calibration equations for both hematite and goethite is presented in Table 2.

For hematite, the equation has a correlation coefficient of 0.992; spectral orange and blue are positively correlated to percent hematite, whereas spectral violet and green have negative coefficients. For goethite, the equation has a correlation coefficient of 0.969; only spectral orange is positively correlated to percent goethite, whereas spectral yellow and red have negative coefficients.

The results of these equations are illustrated in Figure 1 which plots known values for hematite and goethite for our calibration samples (X axis) *vs.* hematite and goethite values estimated from our regression equations (Y axis). In a perfect calibration all samples would lie on a straight line half way between the X and Y axes. While these calibration equations are good, they are not perfect. The hematite equation is clearly better than the goethite equation which tends to overestimate between 0.5 and 1% and underestimate values >1.5%. Nevertheless, the equations do a credible job estimating hematite and goethite in the calibration database.

Test of equations by CBD-extractable Fe

In a typical regression experiment, such as the one being described in this paper, a calibration dataset is used to extract the equations and these equations are tested using a separate test dataset consisting of samples in which the dependent variables are known or have been determined. To test our equations we could put together a test dataset in which we extracted Fe with CBD treatment and then added synthetic hematite and goethite to the CBD-treated samples. A dataset such as this, however, would not indicate how our equations estimate natural Fe oxides. Instead, we have chosen another method of testing, one that makes use of Fe oxides in their natural form.

Our test dataset consists of 41 samples taken about every 40 cm from the top 960 cm of the Luochuan loess section. In each of these samples Fe has been extracted using the CBD extraction technique which removes not only hematite and goethite, but also maghemite and fine-grained magnetite. Our test consists of comparing CBD-

Table 2. Multiple regression statistics and parameter estimates of calibration equations.

		Hematite/dependent variable		
R		R-square		Standard error
0.992		0.985		0.019
Variable	Parameter estimate	Standard error	T	Sig T
Green	−0.0791	0.014	−5.546	0.000
Blue	0.208	0.036	5.800	0.000
Orange	0.103	0.020	5.124	0.000
Violet	−0.0863	0.032	−2.741	0.013
Constant	−1.261	0.663	−1.902	0.072
		Goethite/dependent variable		
R		R-square		Standard error
0.969		0.938		0.148
Variable	Parameter estimate	Standard error	T	Sig T
Constant	−10.60	0.659	−16.108	0.000
Yellow	1.084	0.065	16.546	0.000
Orange	−0.718	0.084	−8.535	0.000
Red	0.340	0.038	8.875	0.000

Note: R = correlation coefficient; T: t-test statistic for null hypothesis that each coefficient is 0; Sig T: significance level for t-test

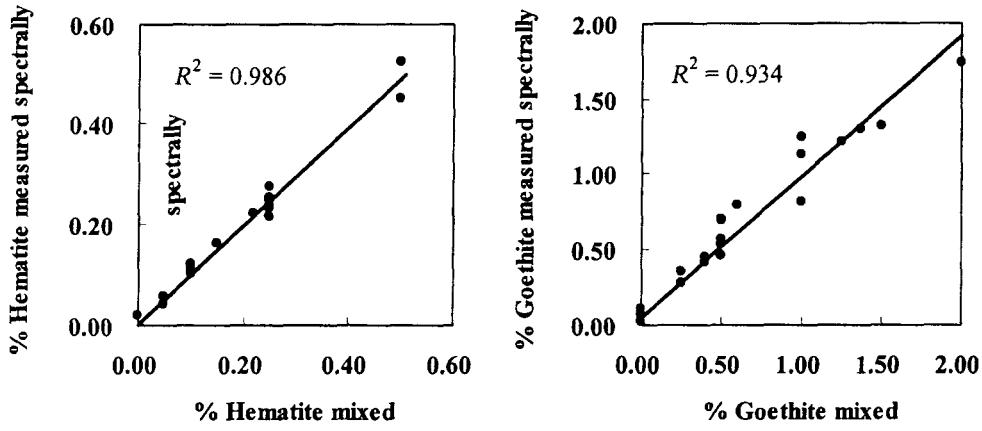

Figure 1. Results of hematite and goethite calibration.

extractable Fe to our spectrally estimated hematite plus goethite. Because pedogenic maghemite and magnetite are present in the loess sequences (Verosub *et al.*, 1993; Fine *et al.*, 1995; Maher, 1998; Liu *et al.*, 1999; Vidic *et al.*, 2000) we expect our estimates to be close to, but always a little less than, CBD-extracted Fe. A comparison of CBD-extracted Fe to estimated hematite plus goethite content (Figure 2) shows an excellent correlation with an R^2 of 0.8867 and, as expected, a consistent pattern of underestimating the CBD-extracted Fe. The underestimate probably results from the combined effects of the CBD extraction removing magnetite and maghemite in addition to hematite and goethite and metals other than Fe substituting into the hematite and goethite structure and changing the color relative to our synthetic samples as noted above. Nevertheless, there is a strong linear relationship (Figure 2) between our spectral data and the CBD-extracted Fe suggesting that the spectral estimates are realistic.

Test of equation for buffering changes in matrix composition

As noted above, the matrix composition differs for loess and paleosol layers, and even for samples from the same loess or paleosol layer. The alternation of loess and paleosol involves a gradual change in the concentration of minerals, such as calcite, clay minerals, quartz, feldspar, *etc.* The most obvious mineral variation from loess to paleosol is the decrease of carbonate, which is leached in the paleosol layers (Liu, 1985). A second major change in mineral composition is the increase of clay minerals, especially illite (Ji *et al.*, 1999), a dark mineral (Balsam *et al.*, 1999) in paleosols. These changes in the composition of loess sediment significantly influence visible spectral bands. In order to buffer our regression equations for the different matrixes present in the loess/paleosol sequence these mineral changes had to be included in our calibration samples.

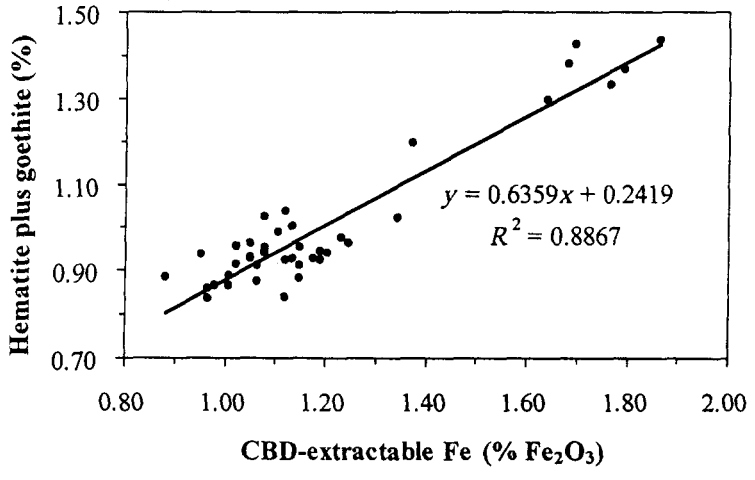

Figure 2. Total hematite plus goethite concentration *vs.* CBD-Fe. Note the difference in *X* and *Y* axis scales.

We have chosen our calibration samples to encompass as much of the mineralogical variation in loess and paleosol as possible thereby increasing the buffering capacity of the calibration equations.

The buffering capacities of the calibration equations were tested in two ways. First, they were applied to the 14 loess-paleosol samples described in Table 3. We determined spectrally the hematite plus goethite concentration, then decalcified the samples, and then determined spectrally the hematite plus goethite concentration on the decalcified samples. If our equations are well buffered, estimates before and after decalcification should be similar. A comparison of the hematite and goethite concentrations for the calcified and decalcified samples exhibits a good correlation suggesting the equation is well buffered for carbonate.

For the second test, typical loess and paleosol samples were chosen and their hematite and goethite concentrations determined spectrally. Then, known concentrations of calcite, quartz, illite, hematite and goethite were mixed with them. The hematite plus goethite concentration of these mixed samples was again determined spectrally (Table 4). For these mixed samples the hematite and goethite concentrations can be calculated from spectrally-estimated hematite and goethite concentrations prior to mixing and the known percentage of Fe oxide minerals admixed. If our equations are well buffered, then the spectrally-estimated hematite and goethite concentrations for the mixed sample should be similar to the calculated concentrations for these same samples. The comparison between the calculated and spectrally estimated hematite and goethite values for the mixture test samples is rather impressive (Table 4), suggesting that our regression equations are sufficiently buffered for changing matrix composition.

Because our calibration equations are derived from the Chinese loess and paleosol samples and the mineral concentrations tested are also based on known concentrations from loess and paleosol, these equations apply only to loess and paleosol. Once the concentration of any of the minerals is exceeded (either in a positive or negative sense) then a 'no analog' situation exists, the equations are extrapolating instead of interpolating, and errors become more likely.

Table 3. Spectrally-determined hematite and goethite concentrations (%) for loess/paleosol before and after decalcification treatments[1].

Depth (cm)	Layer	Magnetic susceptibility[2]	Carbonate (%)	Hematite		Goethite		Hm/Gt[3]	Hm+Gt[3]
				before	after	before	after		
920	S1	166.0	0.6	0.26	0.24	1.17	1.00	0.219	1.43
1180	L2	46.8	12.6	0.18	0.21	0.75	0.92	0.237	0.93
1539	S2	212.6	1.4	0.28	0.28	1.19	1.14	0.234	1.47
1880	L3	61.9	12.7	0.19	0.22	0.82	0.93	0.235	1.01
2101	S3	205.1	6.5	0.28	0.30	1.11	1.15	0.250	1.38
2360	L4	46.2	12.5	0.20	0.23	0.84	0.97	0.235	1.04
2739	S4	217.8	5.0	0.27	0.27	1.17	1.15	0.230	1.44
3060	L5	52.8	14.9	0.20	0.23	0.81	0.95	0.247	1.01
3700	S5	262.1	3.0	0.28	0.29	1.12	1.11	0.247	1.40
4100	L6	33.0	9.4	0.20	0.22	0.81	0.92	0.241	1.01
4420	S6	135.8	1.4	0.28	0.31	1.11	1.17	0.255	1.39
4560	L7	58.0	13.5	0.21	0.25	0.80	1.01	0.262	1.01
4860	S7	132.1	2.7	0.28	0.29	1.09	1.10	0.254	1.37
4960	L8	39.9	17.4	0.18	0.20	0.69	0.79	0.264	0.87
5161	S8	147.1	2.4	0.30	0.32	1.12	1.16	0.264	1.41
5460	L9	22.4	10.4	0.19	0.21	0.84	0.91	0.224	1.03
6237	S9	146.1	1.8	0.29	0.32	1.13	1.09	0.259	1.42
6365	L10	74.8	14.2	0.23	0.27	0.89	1.07	0.255	1.11
6385	S10	120.9	6.9	0.26	0.29	0.99	1.09	0.258	1.25
6485	L11	92.7	10.5	0.24	0.28	0.92	1.06	0.260	1.16
6634	S11	121.3	4.8	0.28	0.29	1.09	1.07	0.259	1.37
6780	L12	81.2	10.6	0.25	0.26	0.93	1.01	0.266	1.18
6879	S12	105.1	5.2	0.29	0.30	1.11	1.11	0.261	1.40
7170	L13	60.1	7.5	0.24	0.26	0.97	0.97	0.249	1.22
7413	S13	153.5	2.3	0.32	0.33	1.12	1.14	0.290	1.44
7580	L14	77.7	8.8	0.25	0.27	0.98	1.03	0.255	1.23
7685	S14	119.6	3.3	0.29	0.32	1.05	1.15	0.277	1.34
7870	L15	22.7	17.6	0.18	0.22	0.73	0.93	0.244	0.90
Loess	Average	55.0	12.3	0.21	0.24	0.84	0.96	0.248	1.05
Paleosol	Average	160.4	3.4	0.28	0.30	1.11	1.12	0.254	1.39

[1] Decalcified by 1 M acetic acid at room temperature
[2] Magnetic susceptibility unit: $10^{-8}m^3kg^{-1}$
[3] Hm = hematite; Gt = goethite, in intact sample

Table 4. Comparison of spectrally-determined with calculated hematite and goethite concentrations for the test mixture samples.

Samples	Hematite		Goethite	
	calculated[1]	determined	calculated[1]	determined
93L902 paleosol		0.26		1.16
93L635 loess		0.16		0.67
5% calcite + 93L902 paleosol	0.25	0.24	1.10	1.08
10% calcite + 93L902 paleosol	0.24	0.24	1.05	1.09
20% illite + 93L635 loess	0.13	0.11	0.56	0.41
5% quartz + 93L635 loess	0.15	0.14	0.64	0.58
5% quartz + 93L902 paleosol	0.25	0.23	1.10	1.01
10% quartz + 93L902 paleosol	0.24	0.22	1.05	0.92
5% Na-feldspar + 93L902 paleosol	0.25	0.24	1.10	1.07
0.1% hematite + 93L635 loess	0.26	0.22	0.67	0.68
0.1% goethite + 93L635 Loess	0.16	0.16	0.77	0.78
0.1% goethite + 93L902 paleosol	0.26	0.25	1.26	1.17
0.5% goethite + 93L902 paleosol	0.26	0.25	1.66	1.39

[1] Calculated hematite and goethite concentrations were derived from the spectrally-determined values of 93L902 paleosol or 93L635 loess and the mixed known percent of mineral, *e.g.* (1) the calculated hematite concentration for 5% calcite + 93L902 paleosol = the determined hematite of 93L902 paleosol /(1+5%); (2) the calculated hematite concentration for 0.1% hematite + 93L635 loess = the determined hematite of 93L635 loess + 0.1%.

Hematite and goethite concentrations in loess and paleosol

The concentration of hematite and goethite in the 14 loess-paleosol pairs is given in Table 3. Both hematite and goethite are high in paleosols and lower in loess. Surprisingly, goethite has a higher concentration not only in loess, as expected, but also in the paleosols. One might expect that the ratio of hematite to goethite (Hm/Gt) would be higher in paleosols than loess because of the red color of the paleosols. On average, the preceding statement is true; the paleosols we analyzed have an average Hm/Gt ratio of 0.254 whereas loess has an average Hm/Gt ratio of 0.248 (Table 3). However, averages can be misleading. In some loess-paleosol pairs the loess actually has a higher Hm/Gt value suggesting that it is the absolute amount of hematite that contributes to the color and not the Hm/Gt ratio. Further, the Hm/Gt ratio exhibits a tendency to increase for both loess and paleosol with depth in the Luochuan section.

Total hematite plus goethite ranges from 0.87 to 1.47%. For paleosols the maximum is 1.47 in S2, the minimum 1.25 in S10 and the average is 1.39. For loess, the maximum is 1.23 in L14, the minimum 0.87 in L8, and the average is 1.05. In paleosols, total hematite plus goethite shows little organized change through the section; hematite plus goethite in loess, however, shows a poorly-defined tendency to increase with depth in the section.

Hematite and goethite are very common in soils, and carry environmental information. On the loess plateau where the soil is uniformly well drained, hematite and goethite concentrations appear to be related to a combination of soil temperature and precipitation (Maher, 1998; Schwertmann and Murad, 1983). Analysis of hematite and goethite concentrations has been hindered by their low concentration in soil and sediments. Reflectance spectroscopy has proved useful for rapid, simple and precise measurement of hematite and goethite in loess and paleosols. Its wider application to other soil and sediment types remains to be explored.

CONCLUSIONS

(1) Visible light diffuse reflectance spectrophotometry is a rapid and precise method of quantifying the absolute concentrations of hematite and goethite in Chinese loess. It is a sensitive and potentially important tool for rapidly and quantitatively analyzing Fe oxide mineral concentrations in other soil and sediment types. (2) The matrix effect, a primary obstacle to estimating the absolute concentration of Fe oxide minerals with the spectral method, can be ameliorated by using the CBD method to remove Fe oxides thereby allowing deferrated loess and paleosol samples to serve as a 'natural' matrix into which known amounts of Fe oxides can be mixed for calibration (standards) samples. (3) By including a variety of different loess and paleosol samples in the regression equations it is possible to overcome the effect of changing matrix from loess to paleosol. These equations apply only to loess and paleosol and once the concentration of any of the minerals is exceeded then a 'no analog' situation exists and errors become more likely. (4) Total hematite plus goethite exhibits a positive correlation to CBD-extractable Fe for the samples studied. In both loess and paleosols, goethite has a greater concentration than hematite. However, both hematite and goethite in paleosols are more concentrated than in loess.

ACKNOWLEDGMENTS

We thank the University of Texas at Arlington, Department of Geology and College of Science for supporting Ji while working in the US (11/99 – 01/00),

and Ms Michele Morrison for making slides and carbonate measurements. This study was funded by NKBRSF Project (G 1999043400) and the National Natural Science Foundation of China (Grants 49725307 and 49873026).

REFERENCES

An, Z.S., Liu T.S., Lou, Y.C., Porter, S.C., Kukla, G., Wu, X.H. and Hua Y.M. (1990) The long-term paleomonsoon variation recorded by the loess-palaeosol sequence in central China. *Quaternary International*, **7/8**, 91–95.

An, Z.S., Kukla, G., Porter, S.C. and Xiao, J.L. (1991) Magnetic susceptibility evidence of monsoon variation on the Loess Plateau of central China during the last 130,000 years. *Quaternary Research*, **36**, 29–36.

Arimoto, R., Balsam, W. and Schloesslin, C. (2000) Visible spectroscopy of atmospheric dust collected on filters: iron-bearing minerals. *Eos Transactions*, AGU, Fall Meeting Supplement, **81**: F69.

Balsam, W.L. and Deaton, B.C. (1991) Sediment dispersal in the Atlantic Ocean: Evaluation by visible light spectra. *Reviews in Aquatic Sciences*, **4**, 411–447.

Balsam, W.L. and Deaton, B.C. (1996) Determining the composition of late Quaternary marine sediments from NUV, VIS and NIR diffuse reflectance spectra. *Marine Geology*, **134**, 31–55.

Balsam, W.L. and Ji, J.F. (1999) Mineralogic variations in the Chinese loess sequence determined by NUV/VIS/NIR reflectance spectra. *GSA Abstracts with Programs*, **31**(7), A-54.

Balsam, W.L. and Wolhart, R. (1993) Sediment dispersal in the Argentine Basin: evidence from visible light spectra. *Deep-Sea Research*, **40**, 1001–1031.

Balsam, W.L., Deaton, B.C. and Damuth, J.E. (1999) Evaluating optical lightness as a proxy for carbonate content in marine sediment cores: Implications for marine sedimentation. *Marine Geology*, **161**, 141–153.

Barranco, F.T., Jr., Balsam, W.L. and Deaton, B.C. (1989) Quantitative reassessment of brick red lutites: Evidence from reflectance spectrophotometry. *Marine Geology*, **89**, 299–314.

Barron, V. and Montealegre, L. (1986) Iron oxides and color of Triassic sediment: Application of the Kubelka-Munk theory. *American Journal of Science*, **286**, 792–802.

Barron, V. and Torrent, J. (1986) Use of the Kubelka-Munk theory to study the influence of iron oxides on soil color. *Journal of Soil Science*, **37**, 499–510.

Bigham, J.M., Golden, D.C., Bowen, L.H., Buol, S.W. and Weed, S.B. (1978) Iron oxide mineralogy of well-drained ultisols and oxisols: I. Characterization of iron oxides in soil clays by Mössbauer spectroscopy, X-ray diffractometry, and selected chemical techniques. *Soil Scicence Society of America Journal*, **42**, 816–825.

Cornell, R.M. and Schwertmann, U. (1996) *The Iron Oxides: Structure, Properties, Reactions, Occurrence and Uses*. Weinheim: VCH Verlagsgesellschaft, 573 pp.

Deaton, B.C. and Balsam, W.L. (1991) Visible spectroscopy – a rapid method for determining hematite and goethite concentration in geological materials. *Journal of Sedimentary Petrology*, **61**, 628–632.

Fernandez, R.N. (1988) Soil color measurements from reflectance spectra: application to the study of iron oxide-soil color relationships. PhD thesis, Purdue University, West Lafayette, 150 pp.

Fine, P., Verosub, K.L. and Singer, M.J. (1995) Pedogenic and lithogenic contributions to the magnetic susceptibility record of the Chinese loess/paleosol sequence. *Geophysical Journal International*, **122**, 97–107.

Harris, S.E. and Mix, A.C. (1999) Pleistocene precipitation balance in the Amazon basin recorded in deep sea sediments. *Quaternary Research*, **51**, 14–26.

Heller, F. and Evans, M.E. (1995) Loess magnetism. *Reviews of Geophysics*, **33**, 211–240.

Heller, F., Shen, C.D., Beer, J., Liu, X.M., Liu, T.S., Bronger, A., Suter, M. and Bonali, G. (1993) Quantitative estimates of pedogenic ferromagnetic mineral formation in Chinese loess and paleoclimatic implications. *Earth and Planetary Science Letters*, **114**, 385–390.

Hunt, C.P., Singer, M.J., Kleteschka, G., TenPas, J. and Verosub, K.L. (1995) Effect of citrate-bicarbonate-dithionite treatment on fine-grained magnetite and maghemite. *Earth and Planetary Science Letters*, **130**, 87–94.

Ji, J.F., Chen, J. and Lu, H.Y. (1999) Origin of illite in the loess from the Luochuan area, Loess Plateau, Central China. *Clay Minerals*, **34**, 525–532.

Jones, G.A. and Kaiteris, P. (1983) A vacuum-gasometric technique for rapid and precise analysis of calcium carbonate in sediments and soils. *Journal of Sedimentary Petrology*, **53**, 655–660.

Judd, D.B. and Wyszecki, G. (1975) *Color in Business, Science, and Industry*. John Wiley & Sons, New York, 553 pp.

Kosmas, C.S., Franzmeier, D.P. and Schulze, D.G. (1986) Relationship among derivative spectroscopy, color, crystallite dimensions, and Al substitution of synthetic goethites and hematites. *Clays and Clay Minerals*, **34**, 625–634.

Kukla, G. and An, Z.S. (1989) Loess stratigraphy in central China. *Palaeogeography, Palaeoclimatology, Palaeoecology*, **72**, 203–225.

Liu, M.X., Hesse, P. and Rolph, T. (1999) Origin of maghaemite in Chinese loess deposits: aeolian or pedogenic. *Physics of the Earth and Planetary Interiors*, **112**, 191–201.

Liu, T.S. (1985) *Loess and the Environment*. China Ocean Press, Beijing.

Maher, B.A. (1998) Magnetic properties of modern soils and Quaternary loessic paleosols: paleoclimatic implications. *Palaeogeography, Palaeoclimatology, Palaeoecology*, **137**, 25–54.

Malengreau, N., Muller, J.-P. and Calas, G. (1994) Fe-speciation in kaolins: A diffuse reflectance study. *Clays and Clay Minerals*, **42**, 137–147.

Mehra, O.P. and Jackson, M.L. (1960) Iron oxide removal from soils and clays by a dithionite-citrate system buffered with sodium bicarbonate. *Clays and Clay Minerals*, **7**, 317–327.

Porter, S. (2000) High-resolution paleoclimatic information form the Chinese eolian sediments based on grayscale intensity profiles. *Quaternary Research*, **53**, 70–77.

Scheinost, A.C. and Schwertmann, U. (1999) Color identification of iron oxides and hydroxysulfates – Use and limitations. *Soil Science Society of America Journal*, **63**, 1463–1471.

Scheinost, A.C., Chavernas, A., Barron, V. and Torrent, J. (1998) Use and limitation of second-derivative diffuse reflectance spectroscopy in the visible to near-infrared range to identify and quantify Fe oxide minerals in soils. *Clays and Clay Minerals*, **46**, 528–536.

Schwertmann, U. and Cornell, R.M. (1991) *Iron Oxides in the Laboratory: Preparation and Characterization*. John Wiley & Sons, New York.

Schwertmann, U. and Murad, E. (1983) Effect of pH on formation of goethite and hematite from ferrihydrite. *Clays and Clay Minerals*, **31**, 277–28.

Torrent, J. and Barron, V. (1993) Laboratory measurements of soil color: theory and practice. Pp. 21–33 in: *Soil Color* (J.M. Bigham and E.J. Ciolkosz, editors). SSSA Special Publication. Soil Science Society of America, Inc., Madison, Wisconsin.

Torrent, J., Schwertmann, U., Fechter, H. and Alferez, F.

(1983) Quantitative relationships between soil color and hematite content. *Soil Science*, **136**, 354–358.

Verosub, K.L., Fine, P., Singer, M.J. and TenPas, J. (1993) Pedogenesis and palaeoclimate: Interpretation of magnetic susceptibility of Chinese loess-palaesol sequences. *Geology*, **21**, 1011–1014.

Vidic, N.J., TenPas, J.D., Verosub, K.L. and Singer, M.J. (2000) Separation of pedogenic and lithogenic components of magnetic susceptibility in the Chinese loess/paleosol sequence as determined by the CBD procedure and a mixing analysis. *Geophysical Journal International*, **142**, 551–562.

(*Received 9 August 2000; revised 22 August 2001; Ms. 477*)